

Supporting Materials for

Twisting Bilayer Graphene Superlattices

Chun-Chieh Lu,¹ Yung-Chang Lin,¹ Zheng Liu,² Chao-Hui Yeh,¹ Kazu Suenaga,² Po-Wen Chiu^{1*}

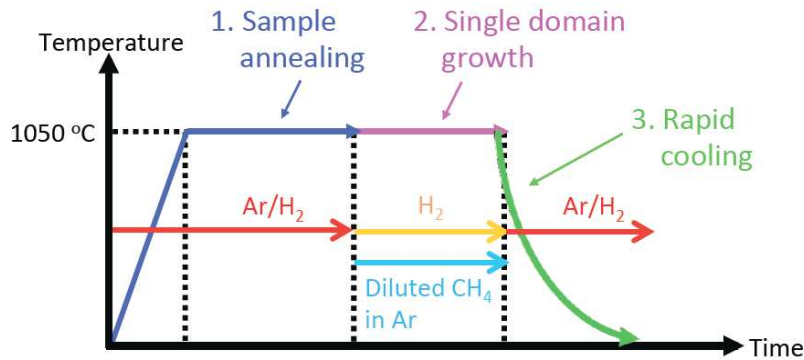
¹Department of Electrical Engineering, National Tsing Hua University, Hsinchu 30013, Taiwan

²National Institute of Advanced Industrial Science and Technology (AIST), Tsukuba 305-8565, Japan

Contents:

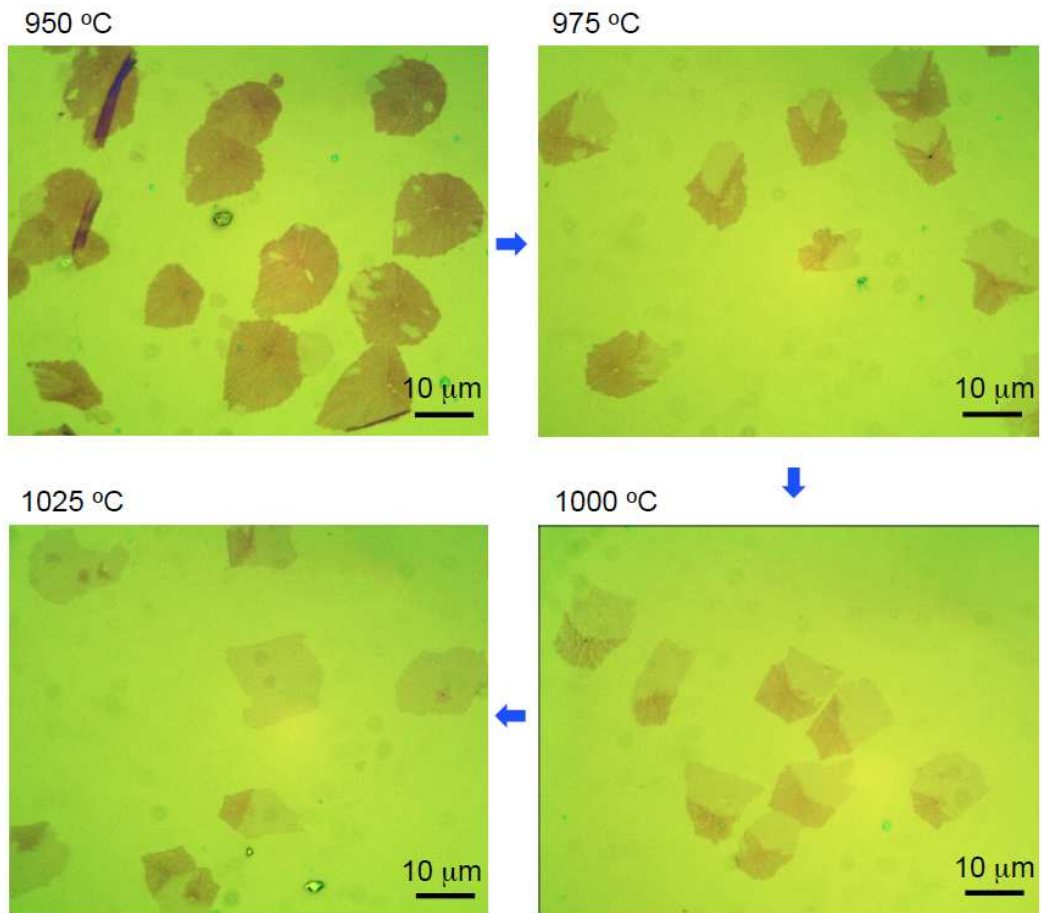
1. CVD temperature vs. time curve
2. AP-CVD parameters: temperature effect
3. AP-CVD parameters: H₂ flow rate
4. AP-CVD parameters: CH₄ flow rate
5. Substrate effect: thickness
6. Uncontrolled BLG growth and nucleation
7. Multiple nucleation of secondary layers
8. Tuning seeded growth: PMMA seeds
9. AFM images of bilayer graphene on silicon substrate
10. Electrical characterizations of single-crystal graphene
11. Process flow of Raman and TEM analysis
12. Large-area HR-TEM image of bilayer graphene superlattice
13. Raman mapping near the D and R peaks

1. CVD temperature vs. time curve



The temperature versus time plot for the AP-CVD growth of bilayer graphene on Cu foil. To grow single-crystal bilayer graphene, the self-limiting CVD reaction was modified by tuning the two growth parameters: concentration of hydrocarbon and temperature. Compared to the growth of single-layer graphene, a higher concentration of hydrocarbon was used to obtain the single-crystal bilayer graphene. First, the Cu foil was mounted in the CVD chamber, and the furnace was ramped up to 1050 °C over 40 min, with 300 s.c.c.m. Ar and 10 s.c.c.m. H₂ flows. After reaching 1050 °C, the sample was annealed for over 90 min without changing the gas flow. For the growth, methane (>80 ppm) mixed with 300 s.c.c.m. Ar and 10 s.c.c.m. H₂ was fed into the reaction chamber for ~7 min to form the bilayer graphene. After the growth, the Cu foil was moved to the cooling zone under the protection of Ar and H₂.

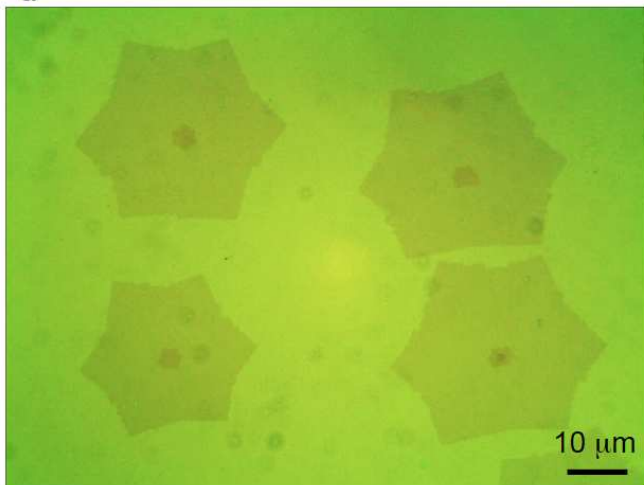
2. AP-CVD parameters: temperature effect



OM images of graphene grains grown on Cu foils at different temperatures, with other growth parameters fixed.

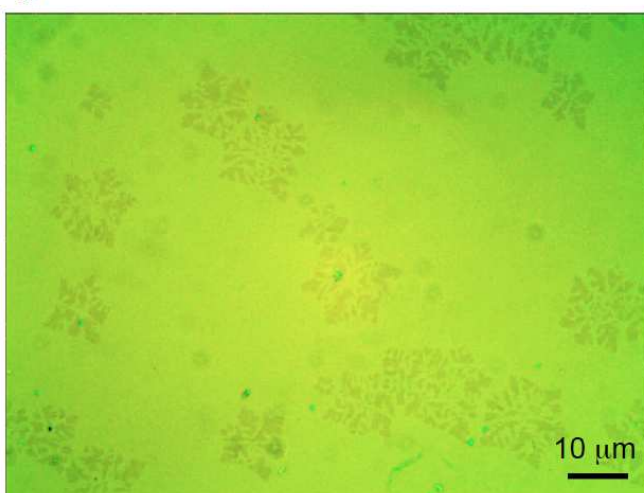
3. AP-CVD parameters: H₂ flow rate

a



CH₄: 300 sccm (80 ppm in Ar)
H₂ : 5 sccm

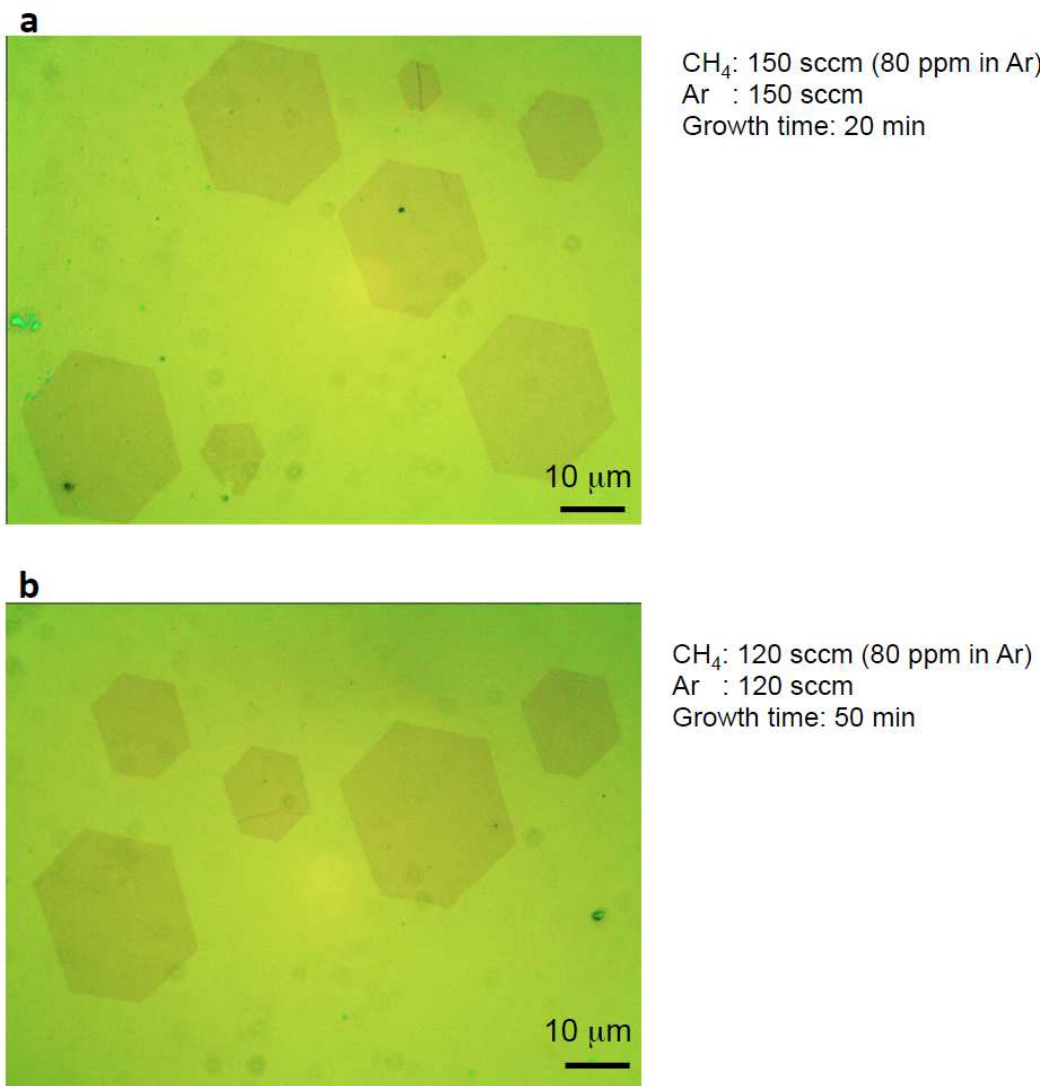
b



CH₄: 300 sccm (80 ppm in Ar)
H₂ : 2 sccm

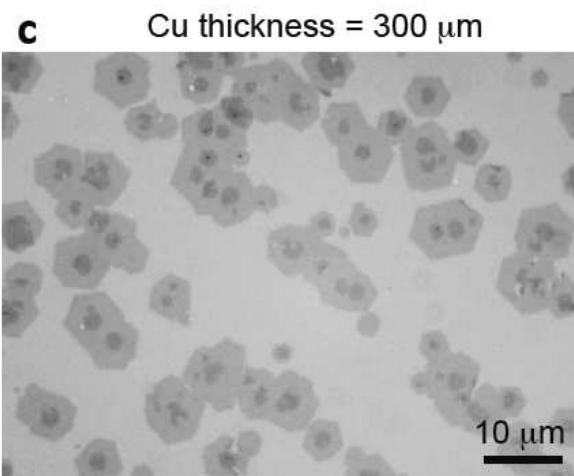
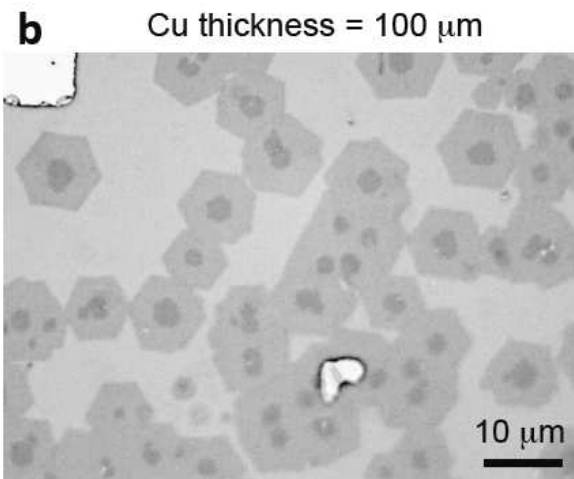
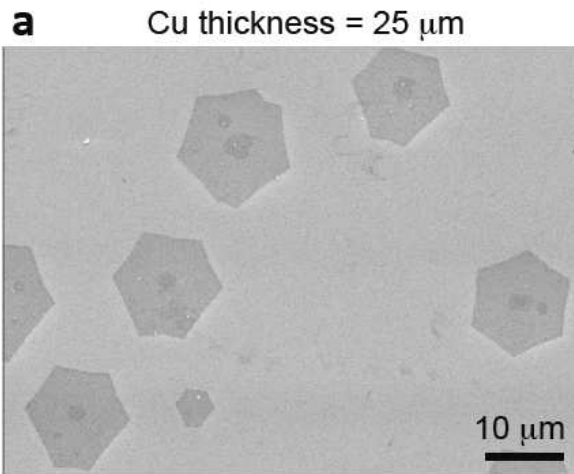
OM images of graphene grains grown on Cu foils at different hydrogen flow rates, with other growth parameters fixed.

4. AP-CVD parameters: CH₄ flow rate



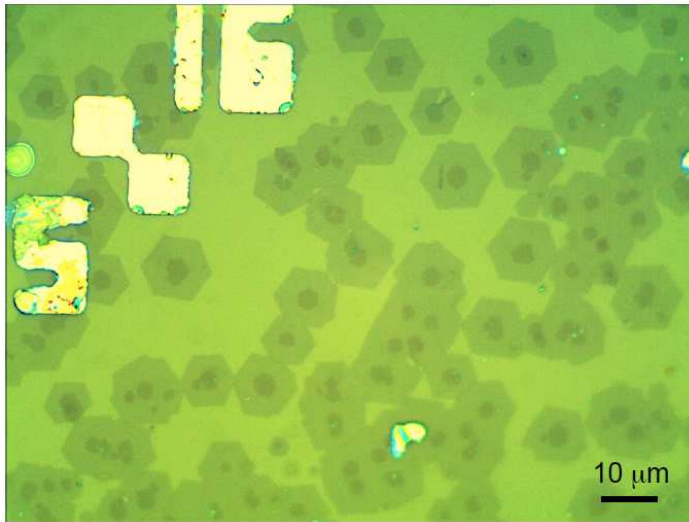
OM images of graphene grains grown on Cu foils at different methane and argon flow rates, with other growth parameters fixed.

5. Substrate effect: thickness



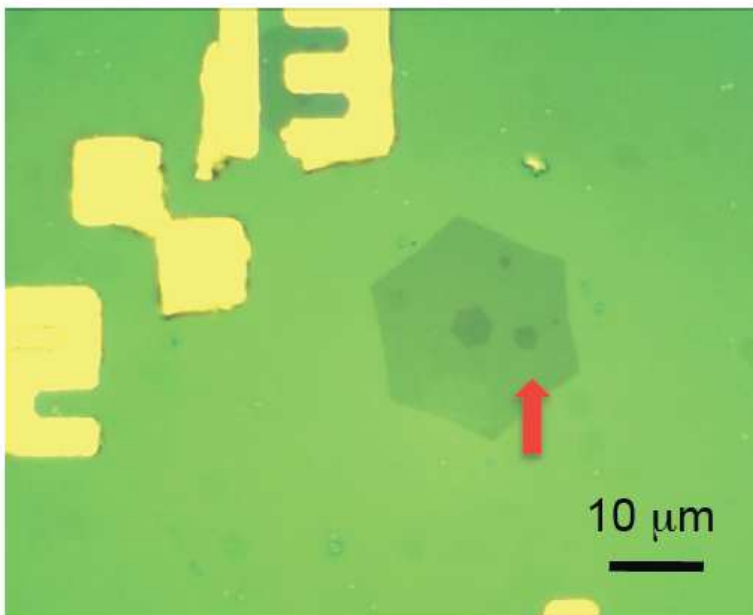
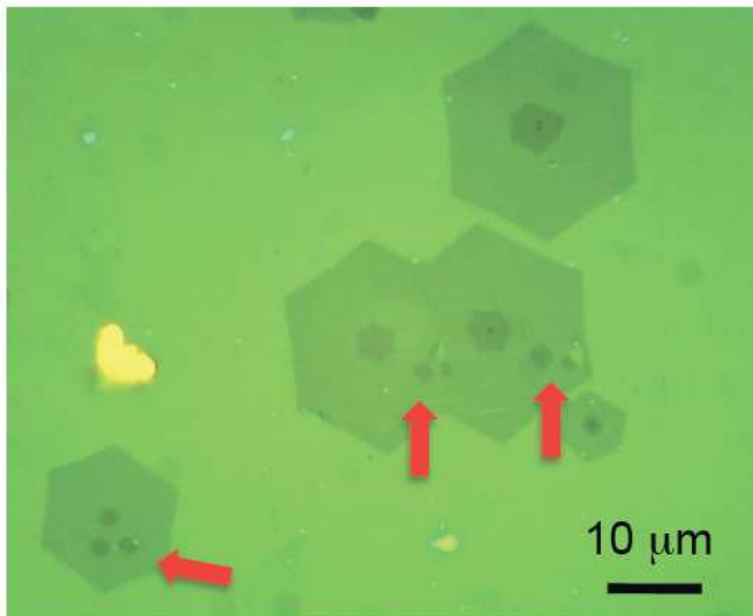
SEM images of graphene grains grown on Cu foils at different thicknesses, with other growth parameters fixed.

6. Uncontrolled BLG growth and nucleation



OM images of graphene grains grown on Cu foils, followed by transfer to a silicon substrate.

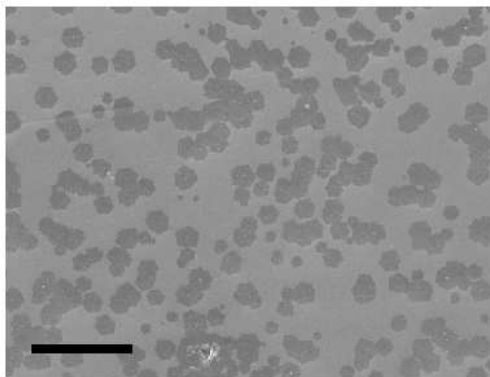
7. Multiple nucleation of secondary layers



OM images of graphene grains grown on Cu foils, followed by transfer to a silicon substrate. The arrows indicate the multiple nucleation of the secondary layers on the host layer.

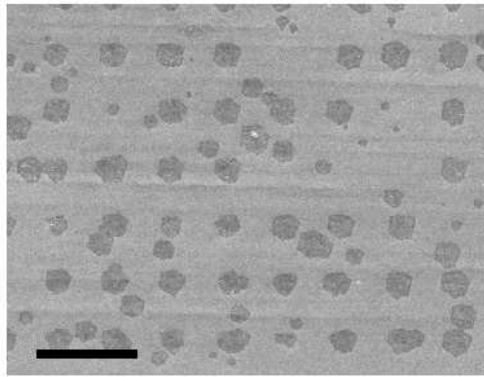
8. Tuning seeded growth: PMMA seeds

a



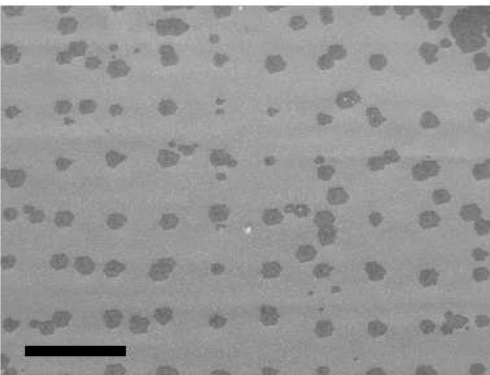
Lower dose
Shorter annealing time

b



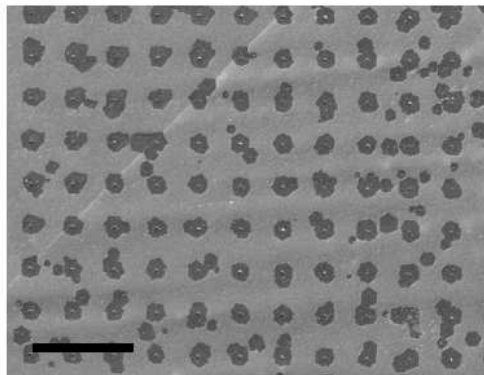
Higher dose
Shorter annealing time

c



Lower dose
Longer annealing time

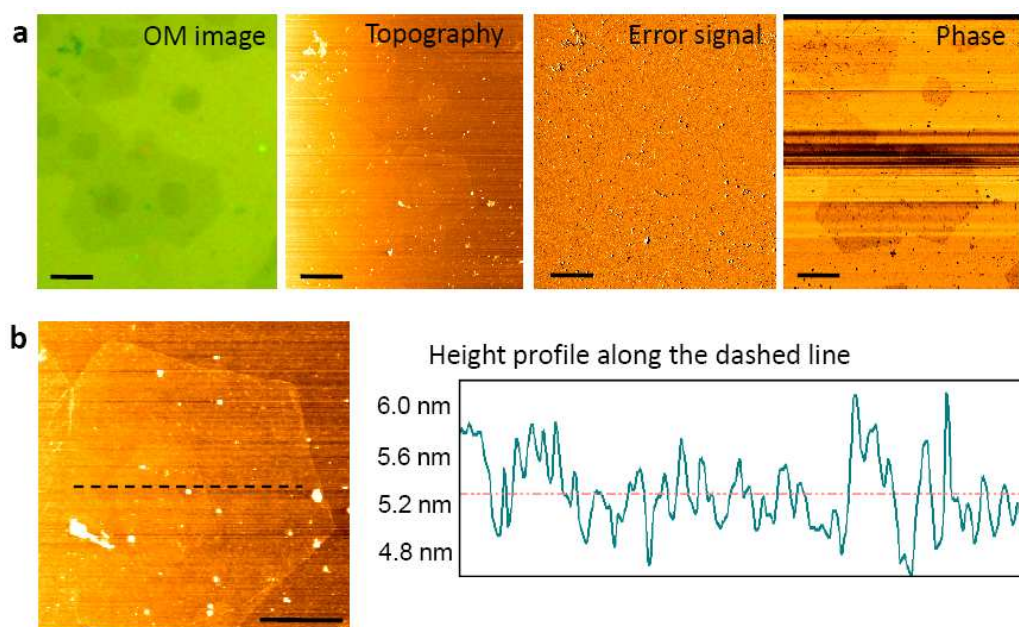
d



Higher dose
Longer annealing time

SEM images of graphene BLG arrays on Cu foils. Cross-linked PMMA is used as seeds. Different thicknesses and dosages are tested. All figures share the same scale bar of 100 μm .

9. AFM images of bilayer graphene on silicon substrate



(a) Optical photograph and atomic force microscopy (AFM) images of the same graphene grain transferred onto a silicon substrate. The AFM images were acquired at ambient conditions using the tapping mode. The AFM phase image shows a relatively clear contrast between the graphene and substrate, but remains difficult to identify the bilayer region. The scale bars of all the images are 5 μm . **(b)** Zoomed AFM topography image of a bilayer graphene grain, with a height profile shown in the right panel of the figure. No clear height step is seen along the scan line indicated in the figure. It is hard to tell whether the central small grain is on the top or at the bottom of the large grain using the AFM technique. The scale bar of the topography image is 2 μm .

10. Electrical characterizations of single-crystal graphene

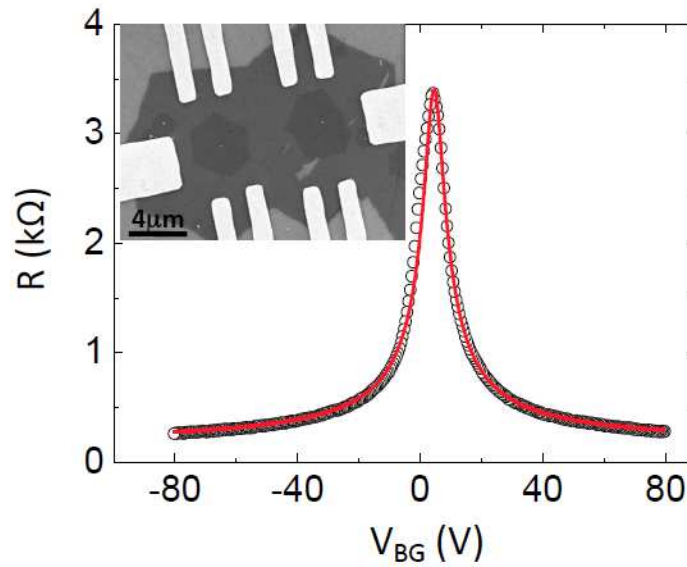
Graphene field-effect transistors were made with e-beam lithography and standard lift-off process on Si chips with 300 nm oxide on top. PMMA in a two-layer structure (996 and 120 K) was spin-coated on the graphene film, followed by baking at 130 °C for 30 min. E-beam lithography was carried out using a scanning electron microscope (JSM-840A) equipped with an e-beam writer (Elphy Quantum, Raith). The exposed PMMA was then developed with methyl isobutyl keton (MIBK) and IPA in a ratio of 1:3. The metal contacts (0.2 nm Cr/30 nm Au) were evaporated following the development. Keithley 2400 and 2000 were, respectively, used as a current/voltage source and multimeter for current–voltage measurements. The R – V_{BG} curves were obtained using the low-frequency (23 Hz) lock-in technique. All the electrical transport measurements were carried out in high vacuum ($\sim 10^{-5}$ torr) at 4 K.

The ambipolar conduction characteristics of graphene provide a rich source of information on its structural perfection, electronic doping and charge scattering. To assess the quality of the graphene layers, we fabricate field-effect transistors in a Hall bar configuration on a degenerately doped silicon substrate with a 300 nm surface. The following figure shows the gate modulation of resistance R as a function of back gate voltage. Whereas R remains $\sim 250 \Omega$ at high carrier density, a sharp peak at $\sim 3.5 \text{ k}\Omega$ appears at the charge neutrality point close to $V_{BG} = 0$. The peak profile is symmetric with respect to the charge neutrality point, indicating a non-doped surface. The full width at half maximum (FWHM) of the peak spans $\sim 11 \text{ V}$ ($\Delta n = 1.3 \times 10^{12} \text{ 1/cm}$) of the back gate voltage which, combined with the high current on/off ratio $I_{on}/I_{off} \approx 14$, indicates the high crystalline quality of the CVD graphene comparable with that obtained by micromechanical cleavage. The intrinsic field-effect mobility is $8000 \text{ cm}^2/\text{V}\cdot\text{s}$, calculated using the formula described in Ref. S1, in which the contact resistance is subtracted in curve fitting. Compared with other CVD

graphene on SiO₂/Si substrates, our results present high electron mobility. We believe that the carrier mobilities of the graphene layers can be further improved using self-assembled molecules as a buffer layer which greatly reduces electron scattering by charged impurities and by surface optical phonons of the silicon substrate^{S2}.

Ref. S1 Kim, S. *et al.* Realization of a high mobility dual-gated graphene field-effect transistor with Al₂O₃ dielectric. *Appl. Phys. Lett.* **94**, 062107 (2009).

Ref. S2 Lafkioti, M. *et al.* Graphene on a hydrophobic substrate: doping reduction and hysteresis suppression under ambient conditions. *Nano Lett.* **10**, 1149-1153 (2010).

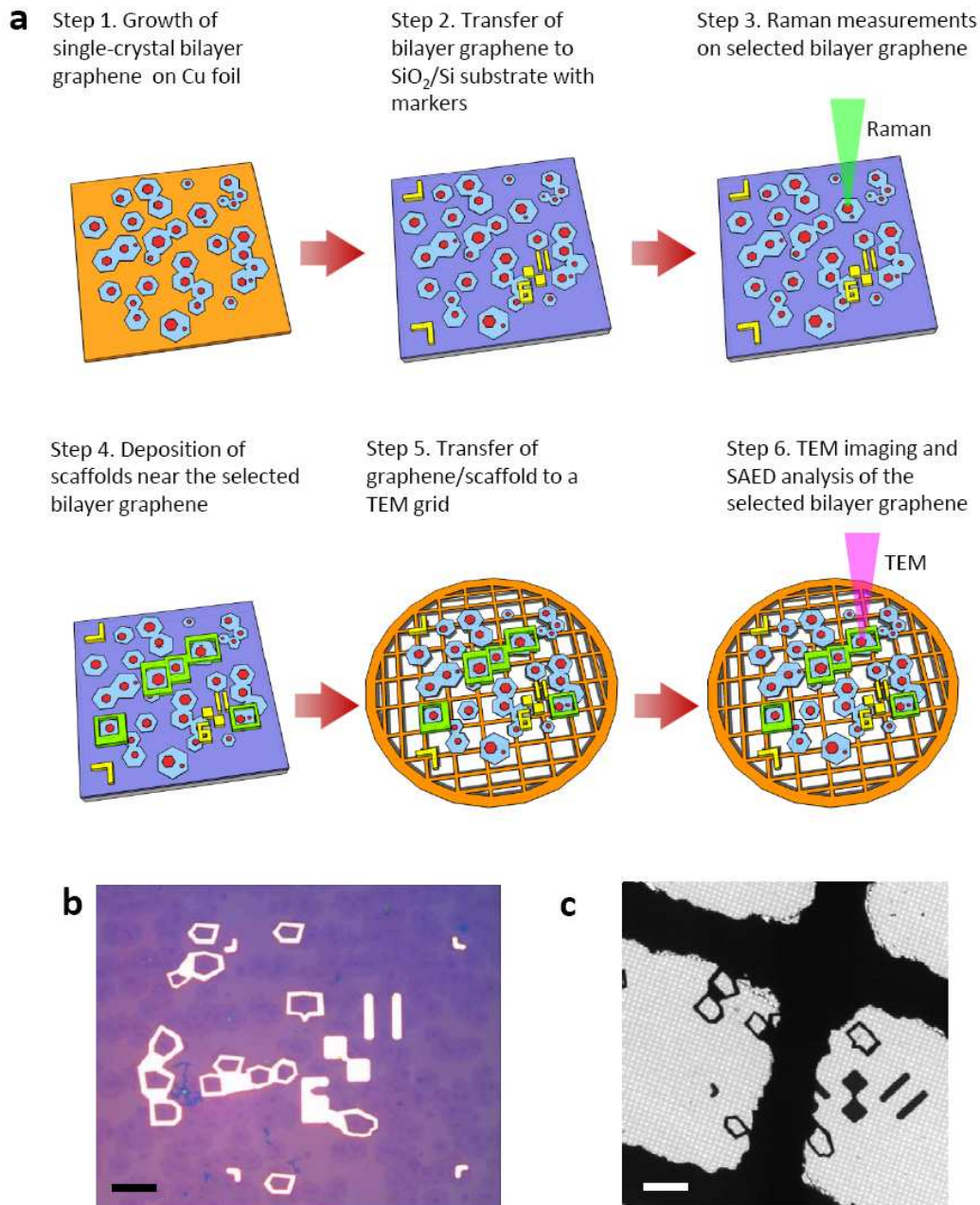


Electrical characterization of grown graphene. a, Resistance as a function of back gate voltage measured in the single-layer region. The solid curve is fit to the following equation to extract the electron mobility μ :

$$R = 2R_C + \frac{L_G}{We\mu \sqrt{n_0^2 + n_G^2}}, \text{ where } R_C \text{ and } n_0 \text{ are the contact resistance and residual}$$

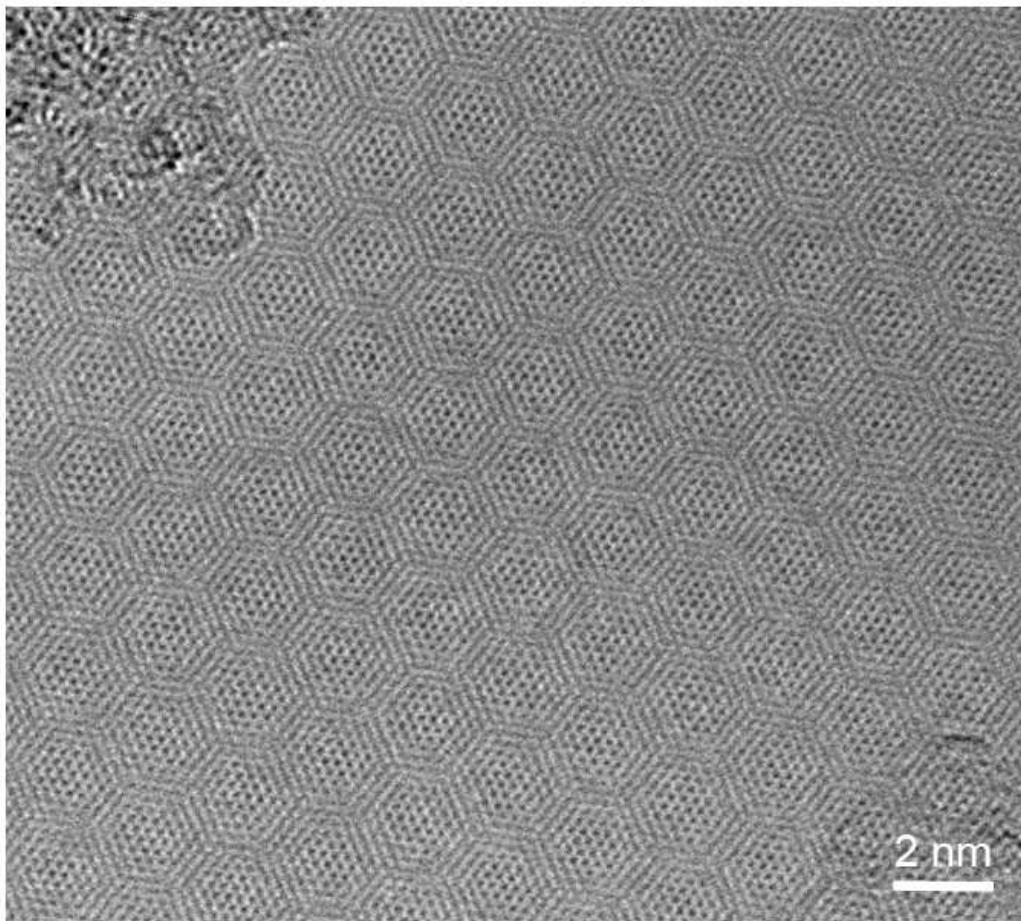
carrier density at the charge neutrality voltage. The geometrical parameters are channel length $L_G = 2 \mu\text{m}$ and channel width $W = 3 \mu\text{m}$.

11. Process flow of Raman and TEM analysis



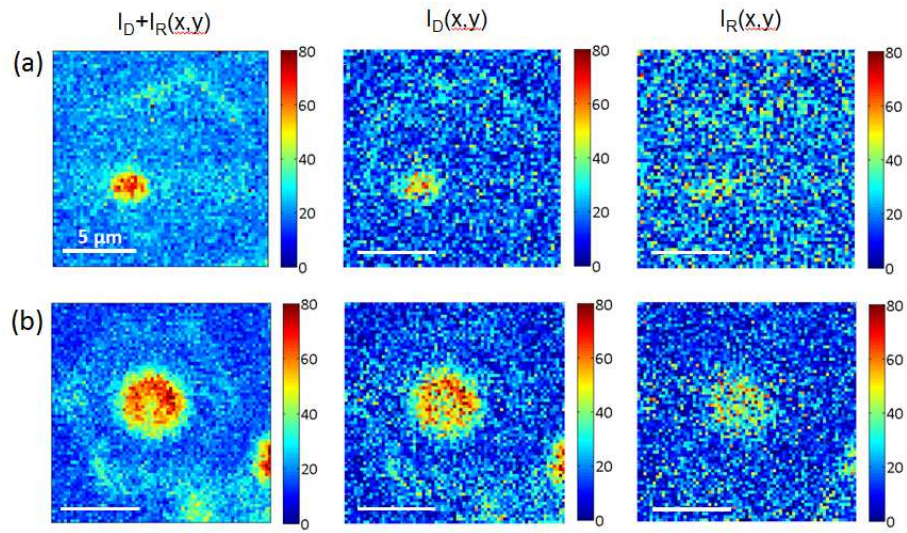
(a) Schematic diagrams illustrating process flow of Raman and TEM analysis. **(b)** Optical photograph of bilayer graphene on silicon substrate with markers and scaffolds. The scale bar is 20 μm . **(c)** Low-magnification TEM image of the same structure transferred onto a Cu grid.

12. Large-area HR-TEM image of bilayer graphene superlattice



The HR-TEM image shows the high crystalline quality of the AP-CVD grown bilayer graphene grains. The Moiré pattern forms as a result of the stacking of two graphene layers.

13. Raman mapping near the D and R peaks



Two-dimensional Raman mappings of BLG shown in Fig. 6 near the D and R peak regions. (a) and (b) are the Raman intensity maps for, respectively, AB stacked and 28° twisted BLG using 488 nm excitation. The spectral regions of the intensity maps are: D ($1355\text{--}1365\text{ cm}^{-1}$) and R peaks ($1370\text{--}1380\text{ cm}^{-1}$). Due to the close frequencies of the two peaks, it is difficult to separate the two peaks clearly.